Neural Networks 22 (2009) 527–535

Contents lists available at ScienceDirect

Neural Networks

journal homepage: www.elsevier.com/locate/neunet

2009 Special Issue

Modulation of LTP/LTD balance in STDP by an activity-dependent feedback mechanism

Shigeru Kubota [a,b,*], Jonathan Rubin [b], Tatsuo Kitajima [c]

[a] Department of Biomedical Information Engineering, Yamagata University, 4-3-16 Jonan, Yonezawa, Yamagata, 992-8510, Japan

[b] Department of Mathematics, University of Pittsburgh, 301 Thackeray Hall, Pittsburgh, PA 15260, USA

[c] Department of Bio-System Engineering, Yamagata University, 4-3-16 Jonan, Yonezawa, Yamagata, 992-8510, Japan

ARTICLE INFO

Article history:
Received 6 May 2009
Received in revised form 25 May 2009
Accepted 25 June 2009

Keywords:
Plasticity
STDP
Synaptic competition
Cortex
Activity-dependent feedback

ABSTRACT

Spike-timing-dependent plasticity (STDP) has been suggested to play a role in the development of functional neuronal connections. However, for STDP to contribute to the synaptic organization, its learning curve should satisfy a requirement that the magnitude of long-term potentiation (LTP) is approximately the same as that of long-term depression (LTD). Without such balance between LTP and LTD, all the synapses are potentiated toward the upper limit or depressed toward the lower limit. Therefore, in this study, we explore the mechanisms by which the LTP/LTD balance in STDP can be modulated adequately. We examine a plasticity model that incorporates an activity-dependent feedback (ADFB) mechanism, wherein LTP induction is suppressed by higher postsynaptic activity. In this model, strengthening an ADFB function gradually decreases the temporal average of the ratio of the magnitude of LTP to that of LTD, whereas enhancing background inhibition augments this ratio. Additionally, correlated inputs can be strengthened or weakened depending on whether the correlation time is shorter or longer than a threshold value, respectively, suggesting that STDP may lead to either Hebbian or anti-Hebbian plasticity outcomes. At an intermediate range of correlation times, the reversal between the two distinct plasticity regimes can occur by changing the level of ADFB modulation and inhibition, providing a physiological mechanism for neurons to select from functionally different forms of learning rules.

1. Introduction

Activity-dependent modification of synaptic transmission, including long-term potentiation (LTP) and long-term depression (LTD), has been widely thought to underlie learning and memory (Bi & Poo, 2001). Although there are various forms of plasticity, recent experiments have revealed that the induction of both LTP and LTD can depend on the relative timing of pre and postsynaptic spikes (Abbott & Nelson, 2000; Bi & Poo, 1998; Caporale & Dan, 2008; Feldman, 2000; Froemke, Poo, & Dan, 2005). In the spike-timing-dependent plasticity (STDP) observed in the neocortical cells, LTP is induced when the presynaptic spike occurs before the postsynaptic spike, while the reversed spike order elicits LTD (Feldman, 2000; Froemke et al., 2005).

An STDP learning rule has been suggested to solve a fundamental problem of unbounded synaptic strengthening in Hebbian learning (Song & Abbott, 2001; Song, Miller, & Abbott, 2000). A Hebbian plasticity rule contributes to the formation of functional circuits and has been used in many neural network studies (Bienenstock, Cooper, & Munro, 1982; Miller, Keller, & Stryker, 1989; von der Malsburg, 1973). However, this plasticity rule predicts that when presynaptic inputs are strengthened, the resulting increased postsynaptic activity further strengthens the inputs. Such positive feedback will lead to unlimited growth of synapses, producing instability in the learning dynamics (Miller, 1996). An advantage of STDP is that it can automatically introduce competitive interaction among inputs to stabilize the postsynaptic activity, while maintaining the basic properties of the Hebbian learning (Abbott & Nelson, 2000; Song et al., 2000). Such competition arises from STDP because the inputs that contribute to rapidly evoking the postsynaptic spikes are potentiated, while the others that do not contribute to it are depressed. However, to achieve such competitive function, LTP and LTD should be approximately balanced in the STDP learning curve such that the maximum level of LTP becomes slightly smaller than that of LTD (Song et al., 2000). When LTP exceeds LTD, all the synapses are potentiated. Conversely, if LTD exceeds LTP to a certain degree, then all the synapses are depressed. The fact that synaptic modification dynamics is quite sensitive to the change in the balance between LTP and LTD (Rubin, Lee, & Sompolinsky, 2001; Song et al., 2000) may suggest that STDP should be

* Corresponding author at: Department of Biomedical Information Engineering, Yamagata University, 4-3-16 Jonan, Yonezawa, Yamagata, 992-8510, Japan. Tel.: +81 238 26 3356; fax: +81 238 26 3299.
E-mail address: kubota@yz.yamagata-u.ac.jp (S. Kubota).

0893-6080/$ – see front matter © 2009 Elsevier Ltd. All rights reserved.
doi:10.1016/j.neunet.2009.06.012

accompanied by an additional mechanism that controls this balance within an adequate range.

Therefore, in this study, we construct a simplified cortical pyramidal neuron model and examine the possible mechanism by which the balance between LTP and LTD in the STDP learning rule can be regulated. Based on the evidence that LTP in STDP depends on postsynaptic NMDA receptors (NMDARs) (Bender, Bender, Brasier, & Feldman, 2006; Egger, Feldmeyer, & Sakmann, 1999; Nevian & Sakmann, 2006), which desensitize via the activity-dependent elevation of intracellular Ca^{2+} (Legendre, Rosenmund, & Westbrook, 1993; Medina, Leinekugel, & Ben-Ari, 1999; Rosenmund, Feltz, & Westbrook, 1995), we examine an STDP model, wherein the magnitude of LTP is dynamically modified by such activity-dependent feedback (ADFB) mechanism (Kubota & Kitajima, 2009; Tegnér & Kepecs, 2002). We show that in this model, the temporal average of the LTP/LTD ratio can be gradually increased or decreased by enhancing the background inhibition or strengthening the feedback function, respectively. In addition, we demonstrate that in the presence of the ADFB function, but not in the absence, input correlations function to potentiate or depress a group of correlated inputs depending on the time scale of the input correlation. Furthermore, in an intermediate range of correlation time, the modulation of the strength of ADFB as well as of inhibition can regulate whether the correlated inputs become strengthened or weakened by STDP, providing neurons with the ability to govern the direction of the input correlation-based plasticity.

2. Methods

2.1. Neuron model

We used a conductance-based pyramidal neuron model consisting of two compartments representing a soma and a dendrite (Kubota & Kitajima, submitted for publication). Both the somatic and dendritic compartments contain voltage-dependent Na^+/K^+ currents (I_{Na} and I_K). A voltage-gated Ca^{2+} current (I_{Ca}) and a Ca^{2+}-dependent potassium current (I_{AHP}) are incorporated into the dendrite to reproduce spike frequency adaptation found in pyramidal cells (Ahmed, Anderson, Douglas, Martin, & Whitteridge, 1998). The amplitude as well as the kinetic parameters for the voltage-gated currents and I_{AHP} have been adjusted such that the model neuron exhibits instantaneous and adapted f–I curves similar to those of neocortical pyramidal cells (Kubota & Kitajima, submitted for publication).

2.2. Synaptic currents

The dendritic compartment receives 4000 excitatory (AMPA and NMDA) and 800 inhibitory (GABA) synapses, each of which follows the conductance-based model given by Kubota and Kitajima (2008) (Fig. 1(A)). The level of inhibitory inputs is assumed to depend on a parameter g_{inh}, which represents the peak conductance of GABA-mediated synaptic currents (Kubota & Kitajima, 2008). All the synapses are activated by Poisson processes. The use of Poisson inputs is based on the experimental finding that the spike trains of *in vivo* cortical cells are highly irregular (Softky & Koch, 1993). Excitatory synapses are activated by either uncorrelated spike trains or two groups of spike trains consisting of correlated and uncorrelated ones, while inhibitory synapses are activated by uncorrelated spike trains. All the uncorrelated inputs were generated using independent Poisson spike trains of 3 Hz. Taking into account a relatively lower success rate of synaptic transmission in central synapses (∼10%) (Hessler, Shirke, & Mallnow, 1993), this input rate corresponds to a presynaptic firing rate of ∼30 Hz, which is in the physiologically plausible range for the sensory-evoked responses of cortical neurons. In cases where the input correlation is considered (Figs. 5 and 6), excitatory synapses are assumed to consist of two equally sized groups (2000 for each group) and one group of synapses is activated by correlated spike trains, while the other group is activated by uncorrelated spike trains (Song & Abbott, 2001). The presynaptic firing rates for the correlated inputs are generated to have a correlation function that decays exponentially with a time constant τ_c (correlation time) (Song & Abbott, 2001; Song et al., 2000). The mean (temporally-averaged) firing rate for the correlated inputs is the same as that for the uncorrelated inputs (3 Hz).

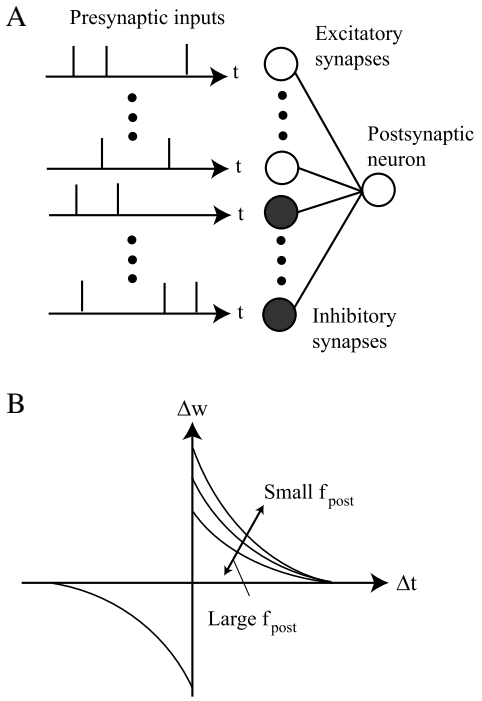

Fig. 1. Components of the computational model. (A) A postsynaptic neuron receives Poisson inputs from both excitatory and inhibitory synapses. The excitatory inputs are plastic and their strength is modified by STDP. (B) The magnitude of LTP in the STDP learning curve is dynamically modulated by feedback depending on postsynaptic firing rate (f_{post}) (Eqs. (1) and (2)).

2.3. Synaptic weight modification by STDP

STDP is assumed to act on all the excitatory (AMPA) synapses. We denote by $\Delta t = t_{post} - t_{pre}$ the time lag between the pre and postsynaptic events; positive numbers of Δt imply that the presynaptic event preceded the postsynaptic event. The change in the synaptic weight Δw is described as follows (Song et al., 2000) (Fig. 1(B)):

$$\Delta w = \begin{cases} A_+ \exp(-\Delta t/\tau_+), & \text{for } \Delta t > 0, \\ -A_- \exp(\Delta t/\tau_-), & \text{for } \Delta t < 0, \end{cases} \quad (1)$$

where A_+ (>0; see below) and A_- (=0.004) determine the magnitude of synaptic potentiation and depression, respectively, and $\tau_+ = \tau_- = 20$ ms determines the temporal range over which synaptic strengthening and weakening occur. The value of A_- corresponds to the relative weight change of 24% when 60 pairs of pre and postsynaptic action potentials take place, as in the case of the physiological experiment of STDP (Froemke et al., 2005). When a pre or postsynaptic event occurs, the synaptic weights w are modified stepwise by an additive updating rule of STDP. The effects of all the pre and postsynaptic spike pairs are linearly summed. Upper and lower bounds (w_{max} and 0, respectively) are imposed on each synaptic weight to stabilize learning dynamics.

2.4. Activity-dependent modulation of LTP

Recent experiments examining STDP (Bender et al., 2006; Egger et al., 1999; Nevian & Sakmann, 2006) have revealed that LTP and LTD involve distinct signaling pathways that may act as coincidence detectors of pre and postsynaptic events: the activation of postsynaptic NMDARs for LTP and that of metabotropic glutamate receptors (mGluRs) for LTD. Further, NMDARs have been shown to exhibit intracellular Ca^{2+}-dependent desensitization (Legendre et al., 1993; Medina et al., 1999; Rosenmund et al., 1995), suggesting that LTP, but not LTD, will be suppressed by sustained postsynaptic activity level that results in the accumulation of intracellular Ca^{2+} (Helmchen, Imoto, & Sakmann, 1996; Svoboda, Denk, Kleinfeld, & Tank, 1997). Therefore, we consider ADFB modulation of plasticity such that increased postsynaptic activity decreases the magnitude of LTP: $A_+(t) = A_+^0 - kf_{post}(t)$, where $f_{post}(t)$ is the postsynaptic firing rate at time t; A_+^0 is the magnitude of LTP when the postsynaptic neuron is almost quiescent (i.e., $f_{post} = 0$); and k (in s) is a positive parameter (see below).

Additionally, a line of evidence suggests that the strength of Ca^{2+}-dependent desensitization of NMDARs may be controlled in cortical neurons. Functional NMDARs are composed of NR1 and NR2 (NR2A–NR2D) subunits in the forebrain (Stephenson, 2001). NR2B-containing NMDARs are predominantly expressed in neonatal neurons, whereas the number of NR2A-containing NMDARs increases over postnatal development (Quinlan, Olstein, & Bear, 1999a; Quinlan, Philpot, Huganir, & Bear, 1999b). Since the NR2A- but not NR2B-containing NMDARs exhibit Ca^{2+}-dependent desensitization (Krupp, Vissel, Heinemann, & Westbrook, 1996), the desensitization can be expected to be facilitated through the NMDAR subunit switch. Moreover, the expression pattern of distinct NR2 subunits is modulated depending on the neuronal activity or the neurotrophin level (Caldeira, Melo, Pereira, Carvalho, Carvalho, & Duarte, 2007; Quinlan et al., 1999a, 1999b), implying that NMDAR subunit composition can alter across different conditions. Therefore, to incorporate the effects of changes in NMDAR subunit expression into our model, we define a non-dimensional parameter ρ ($0 \le \rho \le 1$) such that $\rho = 0$ denotes the state where the NR2B subunits are predominant, as in the case of very immature neurons, whereas $\rho = 1$ represents the state where the NR2A subunits are fully expressed, as in mature neurons. Then, if we denote by $k_{\max}$ the maximum value of the feedback gain parameter k provided by the NR2A-containing NMDARs, the ADFB modulation of the magnitude of LTP (Fig. 1(B)) can be described as

$$A_+(t) = A_+^0 - k_{\max}\rho f_{post}(t). \tag{2}$$

Here, the postsynaptic firing rate at each time point was calculated by $f_{post}(t) = \int_0^\infty \lambda \exp(-\lambda\tau) S_{post}(t-\tau)\mathrm{d}\tau$, with the output spike train represented by $S_{post}(t) = \sum_{t_{post}} \delta(t - t_{post})$ and $\lambda = 0.1/s$ (Tanabe & Pakdaman, 2001). The parameter values used in the ADFB function itself are $A_+^0 = 0.008$ and $k_{\max} = 0.068$ ms. These parameter values were selected such that the postsynaptic firing rate exhibited by our model, including STDP and ADFB, covers a relatively wide range of firing rates observed in neocortical pyramidal cells (60–170 Hz; Fig. 4(D)).

3. Results

3.1. Impact of LTP/LTD balance on learning dynamics by STDP

To investigate how the LTP/LTD balance in the STDP curve affects learning dynamics, we examined the equilibrium properties of the additive STDP rule (i.e., the state where the synaptic weights converge to a stationary distribution) for various values of the LTP size A_+ without ADFB (i.e., $\rho = 0$). In Fig. 2, we plotted the average weight (Fig. 2(A)) and the mean firing rate of the neuron (Fig. 2(B) and (C)) as function of the A_+/A_- ratio for three different values of inhibitory conductance g_{inh}. The figure shows that the equilibrium state of STDP changes abruptly over a small range of A_+/A_- (Rubin et al., 2001; Song et al., 2000): if A_+/A_- is slightly greater than 1, the synaptic weights are increased toward the upper limit so that the postsynaptic firing rate becomes much higher. Conversely, if A_+/A_- becomes less than 0.98, the synapses are strongly depressed and, therefore, the postsynaptic activity becomes much lower. On the other hand, the increased level of inhibition (larger g_{inh}) can gradually decrease the postsynaptic activity for all values of A_+/A_- (Fig. 2(B) and (C)). The finding that the neuronal activity is drastically changed in a very narrow range of A_+/A_- (Fig. 2(C)) implies that to regulate neuronal activity adequately, the LTP/LTD ratio should also be precisely controlled.

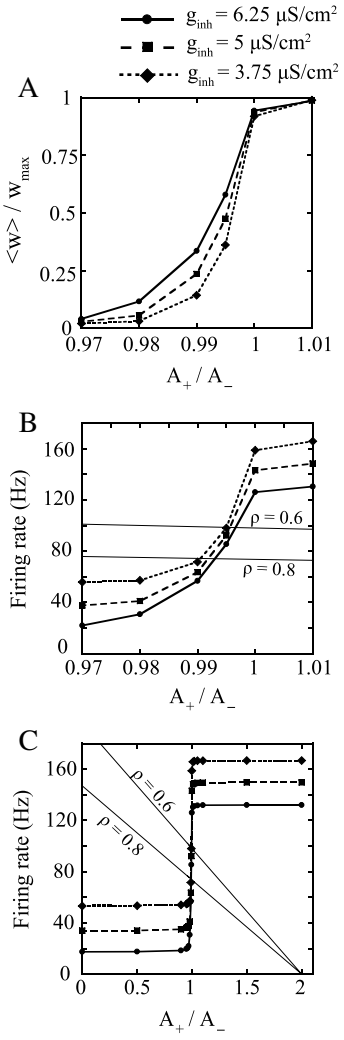

Fig. 2. Predicted effects of changing the LTP/LTD ratio (A_+/A_-) on the equilibrium properties of STDP. Thick lines: The values of average weight (A) and the mean firing rate (B and C), obtained by STDP without ADFB (i.e., $\rho = 0$), were plotted as a function of A_+/A_-, for three different values of the inhibitory conductance g_{inh} ($g_{inh} = 3.75$, 5, or 6.25 μS/cm²). Note that different ranges of A_+/A_- are used in (B) and (C). Thin lines in (B) and (C): The linear relationship between $\overline{A_+/A_-(t)}$ and $\overline{f_{post}(t)}$ specified by Eq. (3) for $\rho = 0.6$ and 0.8.

To explore the possibility that the ADFB mechanism (Eq. (2)) regulates the LTP/LTD ratio, we simply take the temporal average of Eq. (2) to obtain the following relationship:

$$\overline{A_+/A_-(t)} = A_+^0/A_- - \alpha\overline{f_{post}(t)}, \tag{3}$$

Fig. 3. The time course of the A_+/A_- ratio at the equilibrium state of STDP ($\rho = 0.5$ and $g_{inh} = 6.25\ \mu S/cm^2$).

with $\alpha = k_{max}\rho/A_-$. Here, $\overline{x(t)} = T^{-1}\int_t^{t+T} x(t')dt'$ ($T \gg 1$) represents the temporally-averaged value of $x(t)$. Therefore, $\overline{A_+/A_-(t)}$ is the temporal mean of the LTP/LTD ratio and $\overline{f_{post}(t)}$ is the mean firing rate of the postsynaptic neuron. The relationship between $\overline{A_+/A_-(t)}$ and $\overline{f_{post}(t)}$ in Eq. (3) was plotted, for given values of ρ, as shown in Fig. 2(B) and (C) (thin lines). If the temporal fluctuation of A_+/A_- is not so large, it might be expected that the values of $\overline{A_+/A_-(t)}$ and $\overline{f_{post}(t)}$ obtained by STDP, in the presence of ADFB modulation, would correspond to the intersection point between 2 different curves – the line representing Eq. (3) for a given ρ (thin lines) and the postsynaptic rate vs. A_+/A_- curve (thick lines) for a given g_{inh} – in Fig. 2(B).

Note that the increase in the strength of ADFB modulation (larger ρ) will move the intersection point such that the value of A_+/A_- at this point becomes slightly decreased, as can be seen from Fig. 2(B). This implies the possibility that by changing the parameter ρ, the mean value of the A_+/A_- ratio at the equilibrium of STDP might be gradually modified within a very small range of $A_+/A_- \sim 1$. Moreover, Fig. 2(B) also indicates that the enhanced inhibition (larger g_{inh}) would shift the position of the intersection point so that the A_+/A_- ratio becomes slightly increased. Therefore, in the following section, we examine how the changes in the strength of the ADFB mechanism, as well as the background inhibition level, can regulate the LTP/LTD balance in the STDP curve and thereby influence the learning dynamics.

3.2. Control of the LTP/LTD balance through ADFB and inhibitory mechanisms

To explore the role of the ADFB function and inhibition in controlling the LTP/LTD balance, we investigated the equilibrium properties of STDP in the presence of ADFB modulation for various values of ρ and g_{inh}. Since the random synaptic activation, as well as the temporal variation in the synaptic distribution, produces fluctuation in the firing activity, the time course of the A_+/A_- ratio is irregular even at the equilibrium (Fig. 3). However, as the ADFB modulation is facilitated by increasing ρ, the temporally-averaged value of the A_+/A_- ratio was found to converge to a value slightly smaller than 1 (Fig. 4(A) and (B)), as predicted in Fig. 2(B) (Tegnér & Kepecs, 2002). In the presence of this approximate balance in LTP and LTD, a small reduction in the A_+/A_- ratio considerably decreases the average weight as well as the postsynaptic firing rate (Fig. 4(C) and (D)) (Song et al., 2000). Therefore, the strengthening of ADFB by a further increase in ρ is counterbalanced by the weakening of the postsynaptic activity, and the temporal average of A_+/A_- decreases very gradually with increasing ρ (Fig. 4(B)) (Kubota & Kitajima, submitted for publication).

On the other hand, changing g_{inh} does not significantly affect the postsynaptic firing rate for larger ρ ($\rho > 0.4$) (Fig. 4(D)). Instead, stronger inhibition augments the average weight via a small increase in the LTP/LTD ratio (Fig. 4(B) and (C)). This finding suggests that our model exhibits a strong regulatory function that maintains the excitatory–inhibitory balance through the precise control of the LTP/LTD balance. Furthermore, the coefficient of variation (CV) for the interspike intervals (ISIs) in the output spike train was found to increase with ρ and g_{inh} in the range of larger ρ values (Fig. 4(E)). The higher ISI variability caused by the enhanced inhibition is attributable to the fact that larger g_{inh} increases the average synaptic weight (Fig. 4(C)). This effect reduces the number of excitatory inputs needed to reach the threshold voltage and prevent the temporal integration of inputs from producing regular firing pattern (Softky & Koch, 1993). Although larger ρ acts to weaken the synapses (Fig. 4(C)), this effect will be overcome by decreasing the postsynaptic firing rate (Fig. 4(D)); since, at lower firing rates, the effective passive decay for the membrane voltage is increased, the neuron will behave as a coincidence detector and thereby can produce an irregular firing pattern (Liu & Wang, 2001).

Additionally, as shown in Fig. 4(B) and (D) (open symbols), we plotted the values of A_+/A_- and the postsynaptic firing rate corresponding to the intersection points shown in Fig. 2(B) (see Section 3.1), which were calculated by performing the linear interpolation of the firing rate vs. A_+/A_- relationship for each g_{inh} (thick lines in Fig. 2(B)). Fig. 4(B) and (D) indicate that the results obtained by the numerical simulation with the ADFB mechanism (closed symbols) show very good agreement with those predicted by this intersection argument (open symbols).

3.3. ADFB modulation in the presence of correlated inputs

The above results suggest that ADFB may provide STDP with a strong regulatory function such that the postsynaptic firing rate is kept almost constant for a given value of ρ (Fig. 4(D)). To examine how such regulatory action affects learning dynamics in the presence of correlated inputs, we divided synapses into two equally-sized groups and introduced correlation into one of them (Song & Abbott, 2001, see Methods). The other group remained uncorrelated so that we could compare the effects of ADFB on the correlated and uncorrelated inputs.

Physiological experiments examining correlated neuronal activity suggest that the time scale of correlation ranges widely from milliseconds to seconds (Bach & Kruger, 1986; Bair, Zohary, & Newsome, 2001; Brivanlou, Warleand, & Meister, 1998; Kohn & Smith, 2005; Lampl, Reichova, & Ferster, 1999; Mastronarde, 1983; Reich, Mechier, & Victor, 2001); the sharing of the same afferent inputs produces correlated spiking on a millisecond time scale (Mastronarde, 1983), whereas the temporal variation in firing activity caused by changing sensory stimuli can generate correlation on a time scale of seconds (Bach & Kruger, 1986; Bair et al., 2001). Therefore, we performed simulations by using a wide range of correlation time τ_c (5 ms $< \tau_c <$ 5 s), the results of which are presented in Fig. 5(A)–(C). Here, to clarify the impact of ADFB, the results of both using and not using ADFB (left and right column, respectively) are shown. The value of A_+/A_- for the case without ADFB ($A_+/A_- = 0.975$) was chosen such that the steady-state weight distribution becomes approximately the same for the two models with smaller τ_c ($\tau_c = 10$ ms; Fig. 5(A)). As shown in the figure, with such smaller correlation time, the correlated synapses gather near either the upper or lower boundary, whereas the uncorrelated synapses are depressed toward the lower boundary (Song & Abbott, 2001). However, as the correlation time is increased, all the synapses are pushed toward the lower limit in the absence of ADFB (Fig. 5(B), right), converging to a unimodal distribution, whereas in the presence of ADFB, the correlated and uncorrelated inputs tend to decrease and increase, respectively, converging to a bimodal distribution (Fig. 5(B), left). Therefore, in the presence, but not absence of ADFB, there is a threshold value of τ_c such that the correlated inputs are strengthened or weakened, compared to the uncorrelated inputs, depending on whether the value of τ_c is smaller or larger than the threshold, respectively (Fig. 5(C) and (D)).